

A combinatorial approach for determining protease specificities: application to interleukin-1 β converting enzyme (ICE)

Thomas A Rano¹, Tracy Timkey¹, Erin P Peterson², Jennifer Rotonda², Donald W Nicholson³, Joseph W Becker², Kevin T Chapman¹ and Nancy A Thornberry²

Background: Interleukin-1 β converting enzyme (ICE/caspase-1) is the protease responsible for interleukin-1 β (IL-1 β) production in monocytes. It was the first member of a new cysteine protease family to be identified. Members of this family have functions in both inflammation and apoptosis.

Results: A novel method for identifying protease specificity, employing a positional-scanning substrate library, was used to determine the amino-acid preferences of ICE. Using this method, the complete specificity of a protease can be mapped in the time required to perform one assay. The results indicate that the optimal tetrapeptide recognition sequence for ICE is WEHD, not YVAD, as previously believed, and this led to the synthesis of an unusually potent aldehyde inhibitor, Ac-WEHD-CHO ($K_i=56$ pM). The structural basis for this potent inhibition was determined by X-ray crystallography.

Conclusions: The results presented in this study establish a positional-scanning library as a powerful tool for rapidly and accurately assessing protease specificity. The preferred sequence for ICE (WEHD) differs significantly from that found in human pro-interleukin-1 β (YVHD), which suggests that this protease may have additional endogenous substrates, consistent with evidence linking it to apoptosis and IL-1 α production.

Addresses: ¹Department of Molecular Design and Diversity, Merck Research Laboratories, R123-232, PO Box 2000, Rahway, New Jersey 07065, USA, ²Department of Biochemistry, Merck Research Laboratories, R80W-250, PO Box 2000, Rahway, New Jersey 07065, USA and ³Department of Biochemistry and Molecular Biology, Merck Frosst Centre for Therapeutic Research, PO Box 1005, Pointe Claire - Dorval, Quebec, Canada H9R 4P8.

Correspondence: KT Chapman or NA Thornberry

Key words: caspase, cysteine protease, ICE, positional scanning, specificity

Received: 22 January 1997

Accepted: 7 February 1997

Electronic identifier: 1074-5521-004-00149

Chemistry & Biology February 1997, 4:149-155

© Current Biology Ltd ISSN 1074-5521

Introduction

A detailed knowledge of the specificity of a particular protease can provide clues to its biological function(s), and is invaluable for designing appropriate peptide-based substrates and potent, selective inhibitors. Traditionally, most investigations of protease specificity have required the synthesis of large numbers of peptides and/or peptide-based inhibitors, which were analyzed individually for cleavage or inhibition. More recently, several investigators have developed more efficient techniques for determining protease specificity, including substrate phage display [1-3], methods for rapid analysis of peptide mixtures [4-6], and use of peptide nucleophiles [7].

Positional-scanning synthetic combinatorial libraries (PS-SCL) [8] have recently emerged as a powerful method for rapidly identifying high-affinity peptide sequences from a mixture of compounds. Peptide-based PS-SCLs are generally composed of several sub-libraries in which one position is defined with an amino acid, and the remaining positions contain a mixture of amino acids present in approximately equimolar concentrations [9]. Analysis of the library will identify the preferred amino acids for each position. Such libraries have been successfully employed for the identification of potent receptor ligands [10,11], enzyme inhibitors [12-15], and specific

antigens [8,16], but have not yet been used to determine protease specificity.

Here we describe a novel PS-SCL designed to investigate the specificity of interleukin-1 β converting enzyme (ICE/caspase-1, EC 3.4.22.36), the cysteine protease responsible for the production of IL-1 β in monocytes [17-22]. Since its discovery in 1989 [17,18], this enzyme has been the subject of intense interest as a potential therapeutic target for the treatment of inflammatory diseases. The finding that ICE-deficient mice are resistant to lipopolysaccharide-induced endotoxic shock supports the hypothesis that this enzyme is a key mediator of inflammation [21,22]. Surprisingly, these mice are defective not only in IL-1 β ; their ability to make mature IL-1 α is also impaired, suggesting that this enzyme has multiple biological functions.

ICE is the first identified member of a new cysteine protease family that includes CED-3, the product of a gene required for programmed cell death in the nematode *Caenorhabditis elegans* [23]. The ICE/CED-3 or caspase family [24] currently includes ten human proteases. Although it appears that at least some of the caspases closely related to CED-3 are involved in mammalian cell death [25], a prominent role for ICE has not

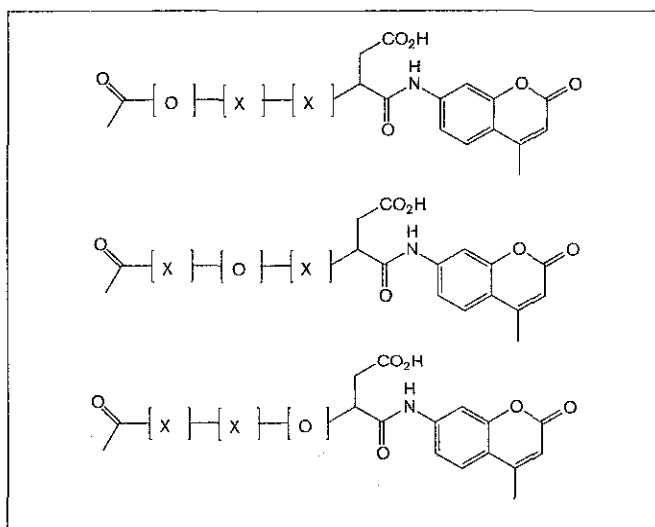
been established. In particular, ICE-deficient mice are not significantly defective in apoptosis, suggesting that this caspase is not essential for this process [21,22].

Results

Positional-scanning substrate library

In order to have a better understanding of the biological function(s) of ICE, and to aid the development of selective inhibitors, the peptide substrate specificity of ICE was determined in detail using a PS-SCL with the general structure Ac-X-X-X-Asp-aminomethylcoumarin (AMC) (Fig. 1). This library was designed on the basis of several catalytic properties of this enzyme. First, its most distinctive feature is a near absolute requirement for aspartic acid in the position to the immediate left of the scissile bond (P_1) of both peptide and macromolecular substrates [20,26,27]. Second, there is an equally stringent requirement for four amino acids on the amino-terminal side of the scissile bond [20]. Finally, tetrapeptides terminating in -Asp-AMC are highly sensitive fluorogenic substrates for this enzyme [20,28], being specifically cleaved after Asp to liberate the fluorescent leaving group, AMC. The particular PS-SCL described here consists of three separate sub-libraries that are each composed of 8000 compounds. In each sub-library, 'X' represents the mixture of amino acids (excluding cysteine and methionine) and 'O' represents the spatially addressed amino acids. Using this strategy, analysis of the three sub-libraries (20 samples each) affords

Figure 1



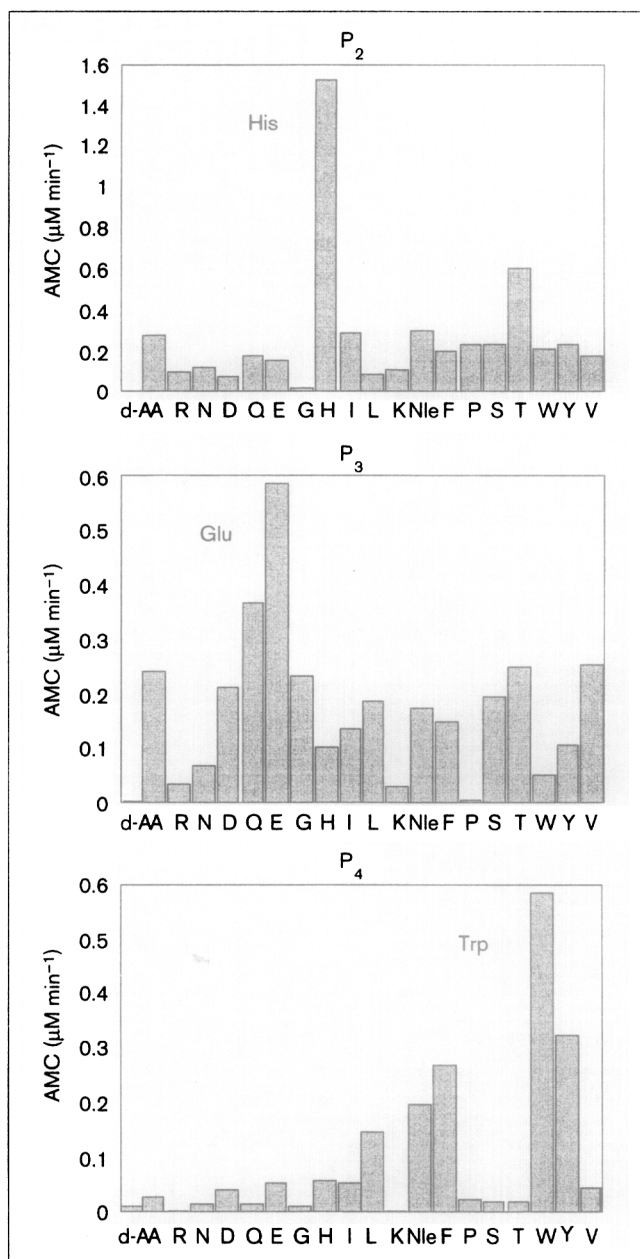
Tetrapeptide-AMC combinatorial positional-scanning library. The positional-scanning library consists of 3 separate sub-libraries of 8000 compounds each (20 wells of 400 compounds). Each library is comprised of an amino-terminal acylated tetrapeptide-aminomethylcoumarin derivative, where 'X' represents the isokinetic mixture of proteogenic amino acids and 'O' represents the spatially addressed proteogenic amino acids (excluding cysteine and methionine).

a complete understanding of the amino acid preferences across S_2 , S_3 and S_4 subsites.

The optimal peptide recognition sequence for ICE

The substrate specificity of ICE determined with the PS-SCL indicates that the optimal tetrapeptide recognition

Figure 2



Substrate specificity of ICE. To determine protease specificity, enzyme was added to reaction mixtures containing 100 μ M substrate mix, 100 mM Hepes, 10 mM DTT, pH 7.5 in a total volume of 100 μ l. Under these conditions the final concentration of each individual compound is approximately 0.25 μ M. Production of AMC was monitored continuously at ambient temperature in a Tecan Fluostar 96-well plate reader using an excitation wavelength of 380 nm and an emission wavelength of 460 nm.

Table 1**Comparison of fluorogenic substrates for ICE.**

Substrate	$10^{-5} \times k_{\text{cat}}/K_m$ ($M^{-1}s^{-1}$)
Ac-WEHD-AMC	33.4 ± 0.3
Ac-WVHD-AMC	15.7 ± 0.1
Ac-YEHD-AMC	9.56 ± 0.20
Ac-WEAD-AMC	7.55 ± 0.07
Ac-YVHD-AMC	2.81 ± 0.14
Ac-WVAD-AMC	2.41 ± 0.60
Ac-YEAD-AMC	1.85 ± 0.07
Ac-YVAD-AMC	0.66 ± 0.14
pro-IL-1 β	1.5

motif for this enzyme is Trp-Glu-His-Asp (WEHD) (Fig. 2). Hydrophobic amino acids are preferred in S_4 (Trp > Tyr > nor-Leu > Leu), liberal substitutions are tolerated in S_3 and His is favored by approximately threefold over Thr in S_2 . The finding that WEHD is the optimal tetrapeptide sequence for ICE was surprising for two reasons. First, it differs significantly from the P_4 - P_1 amino acids in human pro-IL-1 β , Tyr-Val-His-Asp (YVHD). Second, previous studies of specificity [29] had suggested that the optimal sequence for the enzyme was Tyr-Val-Ala-Asp (YVAD).

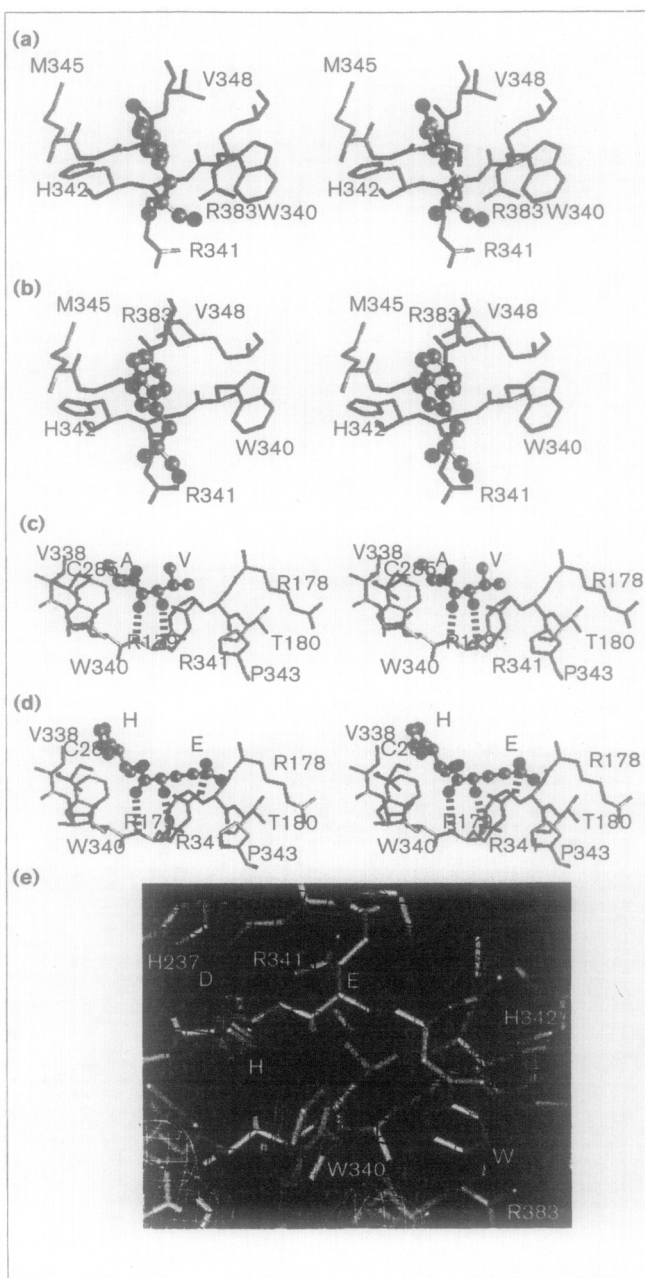
To confirm that WEHD is, in fact, the preferred tetrapeptide recognition motif, and to confirm that this approach provides an accurate measure of protease specificity, a series of fluorogenic substrates containing all possible combinations of the amino acids in WEHD and YVAD was synthesized and tested for cleavage by ICE. The results, shown in Table 1, indicate that k_{cat}/K_m for cleavage of Ac-WEHD-AMC ($3.3 \times 10^6 M^{-1}s^{-1}$) is 50-fold higher than that for Ac-YVAD-AMC ($0.066 \times 10^6 M^{-1}s^{-1}$) and 22-fold higher than that for pro-IL-1 β ($1.5 \times 10^5 M^{-1}s^{-1}$, [28]). Moreover, the enzyme's order of preference for the eight substrates is perfectly predicted by the library. Consistent with these findings, incorporation of WEHD into pro-IL-1 β results in an approximately six-fold increase in k_{cat}/K_m (data not shown). The finding that the tetrapeptide in pro-IL-1 β is not optimal for this enzyme suggests that ICE may have additional endogenous substrates.

Inhibition of ICE by Ac-WEHD-CHO

Upon discovering that the preferred substrate for ICE is Ac-WEHD-AMC, the corresponding tetrapeptide

Table 2**Inhibition of ICE by peptide aldehydes.**

	k_{on} ($M^{-1}s^{-1}$)	k_{off} (s^{-1})	K_i (nM)
Ac-YVAD-CHO	3.8×10^5	2.9×10^{-4}	760
Ac-WEHD-CHO	2.6×10^5	1.5×10^{-5}	56
Selectivity			14-fold

Figure 3

Stereo diagrams of the S_4 subsites of (a) ICE•Ac-YVAD-CHO and (b) ICE•Ac-WEHD-CHO and the S_2 and S_3 subsites of (c) ICE•Ac-YVAD-CHO and (d) ICE•Ac-WEHD-CHO. Protein groups are represented as a stick model and the bound inhibitors as ball-and-stick models. Representative groups are labeled, residues of the inhibitor are indicated with the one-letter code in (c) and (d), and polar interactions are drawn as dashed lines. (e) Electron density in the vicinity of the bound Ac-WEHD-CHO inhibitors. The model is displayed together with density from the final ($2F_o - F_c$) map. Residues in the inhibitor are identified with the one-letter code, and residues in the protein by one-letter code and amino-acid sequences number. Panels (a-d) were prepared with C-View (J.C. Culbertson, Merck Research Laboratories); panel (e) was prepared with QUANTA (Molecular simulations, San Diego, USA).

aldehyde was synthesized and tested, in anticipation that it would be a more potent peptide-based inhibitor than those previously described for this enzyme. Peptide aldehydes are effective, competitive, reversible inhibitors of cysteine proteases, forming a thiohemiacetal with the active site cysteine (for review, see [30]). Inhibition of ICE by Ac-WEHD-CHO is characterized by a relatively slow association rate constant, $2.6 \times 10^5 \text{ M}^{-1}\text{s}^{-1}$, and a dissociation rate constant of $1.5 \times 10^{-5} \text{ s}^{-1}$, corresponding to an overall dissociation constant ($K_i = k_{\text{off}}/k_{\text{on}}$) of 56 pM, making it among the most potent reversible inhibitors described for any caspase. This represents an improvement in binding affinity of 14-fold over Ac-YVAD-CHO, the compound previously thought to be the best peptide-based, reversible inhibitor of ICE. Ac-WEHD-CHO is a more potent inhibitor than Ac-YVAD-CHO because there is an increase in the lifetime of the enzyme-inhibitor complex ($t_{1/2 \text{ YVAD}} = 0.66 \text{ h}$, $t_{1/2 \text{ WEHD}} = 12.8 \text{ h}$) (Table 2).

Three-dimensional structure of ICE•Ac-WEHD-CHO

To understand the structural basis of the improved affinity of Ac-WEHD-CHO, the three-dimensional structure of the ICE•Ac-WEHD-CHO complex was determined by X-ray crystallography, and is compared to that of ICE•Ac-YVAD-CHO [31,32] in Figure 3. The overall structures of the two complexes are, in many ways, quite similar. The same three mainchain hydrogen bonds are formed ($\text{P}_1\text{N}-\text{Scr}^{339}\text{O}$, $\text{P}_3\text{N}-\text{Arg}^{341}\text{O}$ and $\text{P}_3\text{O}-\text{Arg}^{341}\text{N}$) and comparable interactions are involved in the stabilization of the P_1 Asp. In addition, in both structures the chiral center of the hemithioacetal is predominantly in the nontransition state configuration, allowing the hydroxyl group to make a polar interaction with the sidechain of the catalytic His²³⁷. In contrast to these similarities, and despite the relatively low resolution (2.7 Å) of these studies, there are clear differences in the protein-inhibitor interactions in the S_2 , S_3 and S_4 subsites that appear to account for the increased potency of Ac-WEHD-CHO. First, in both structures the aromatic sidechain contacts the imidazole ring of His³⁴² in S_4 . In the ICE•Ac-WEHD-CHO crystal, however, the sidechain of Arg³⁸³ is rotated away from the conformation seen in the YVAD complex and into a position that would allow a favorable interaction with the partial negative center of the P_4 Trp (Fig. 3a,b). Second, in S_3 , increased binding energy apparently comes from a salt link between the carboxylate of the P_3 Glu and the $\text{N}^{\eta 2}$ of Arg³⁴¹ (Fig. 3c,d). Finally, additional binding energy in S_2 appears to arise from a relationship between the inhibitor's histidyl sidechain and Trp³⁴⁰ (Fig. 3d). The $\text{N}^{\epsilon 2}$ atom of the imidazole is appropriately positioned to make a favorable interaction with the partial charges on both the $\text{C}^{\eta 2}$ and $\text{C}^{\zeta 3}$ atoms of the indole sidechain.

Discussion

The results presented in this study establish that a PS-SCL is a powerful tool for rapidly and accurately

assessing protease specificity. Using this approach, the amino-acid preferences of all subsites can be determined simultaneously, in the time required to perform one assay. This is therefore an economic method, requiring only catalytic quantities of enzyme. The results obtained with ICE indicated that the preferred tetrapeptide recognition motif is WEHD, not YVAD, as previously believed. Therefore, to demonstrate the validity of this approach Ac-WEHD-AMC was synthesized and found to have a second-order rate constant (k_{cat}/K_m) of $3.3 \times 10^6 \text{ M}^{-1}\text{s}^{-1}$ that is 50-fold higher than that for Ac-YVAD-AMC. This knowledge was in turn extended to inhibitor design; Ac-WEHD-CHO is the most potent reversible, small-molecule inhibitor described for any of the caspases ($K_i = 56 \text{ pM}$). By analogy with Ac-YVAD-CHO, the degree of hydration of Ac-WEHD-CHO is expected to be approximately 90%. Thus, the intrinsic K_i for this compound is likely to be $<10 \text{ pM}$.

Previously, the specificity of ICE was determined using a series of hexapeptides obtained by making single amino-acid substitutions in the parent peptide Ac-YVADGW-NH₂ [32]. The results from this study indicated that the preferred recognition motif for ICE is YVAD, which closely matches the corresponding sequence in human pro-IL-1 β , YVHD. The discrepancies between the results presented here, and those published earlier, are in part because only a subset of amino acids was employed in the first study. For example, Trp was not substituted in the P_4 position of the hexapeptide. There is, however, a fundamental difference between the two methods which can account for difference in the results. In the earlier study, substitutions at one position were explored while the other positions contained fixed amino acids. The results from such an experiment are no doubt greatly influenced by the identity of the amino acids at the nonsubstituted positions. In contrast, in the current study, one position is varied while the other positions contain a mixture of amino acids present in approximately equimolar concentrations. The finding that Ac-WEHD-AMC is cleaved 50-fold more efficiently than Ac-YVAD-AMD indicates that the method used here gives a more accurate description of protease specificity.

The PS-SCL described in this study clearly could also be used for determining the specificities of other caspases. It was designed on the basis of several catalytic features that appear to be conserved among all known ICE homologs, including a near absolute requirement for Asp in the S_1 subsite and an ability to accommodate large hydrophobic groups (e.g. AMC) in the prime sites. To date, we have mapped the specificities of 9 of the 10 known caspases, and the cytotoxic lymphocyte-derived serine protease, granzyme B, an enzyme that also has the ability to cleave after Asp (data not shown).

This is the first example of a PS-SCL that has been used to determine protease specificity. Presumably, this

approach has not been more broadly applied for this purpose because of the difficulty involved in measuring hydrolysis rates of peptides in mixtures. Using the strategy employed here, in which a fluorescent leaving group is incorporated in the P₁' position, reaction rates are measured simply by following an increase in fluorescence. The results suggest that an analogous library in which the P₁ position is also varied (Ac-X-X-X-AMC) would be invaluable for determining the specificity of many cysteine and serine proteases; in general these enzymes have the ability to cleave peptide analogs containing a photometric leaving group in P₁'.

The results presented here show that the sequence in human pro-IL-1 β that is cleaved to generate the mature, biologically active cytokine, YVHD¹¹⁶-A¹¹⁷, is not optimal for ICE. Its preferred tetrapeptide, WEHD, more closely resembles the evolutionarily conserved upstream site in pro-IL-1 β that is also cleaved by this enzyme, FEAD²⁷-G²⁸ [17,18]. Nonetheless, the observation that neither of these sequences is optimal for ICE, together with the finding the optimal sequence for caspase-3 (DEVD) is identical to the cleavage sites in known endogenous substrates for this enzyme (data not shown), suggests that ICE may have multiple biological functions, which is consistent with evidence linking it to apoptosis and IL-1 α production [21,22]. One possible function is suggested by the finding that ICE and closely related homologs (caspase-4 and caspase-5) all appear to be activated via cleavage at a WXXD sequence; ICE may be one component of a proteolytic cascade that is triggered in response to inflammatory stimuli, resulting in the production of both IL-1 β and IL-1 α .

Significance

The methods traditionally used for studies of protease specificity are generally tedious, and often produce an incomplete analysis of specificity. The approach described here, using a positional-scanning combinatorial substrate library, enables a rapid, accurate and rigorous analysis of protease specificity using catalytic quantities of enzyme. This novel method could be used for specificity studies of a variety of proteases, and possibly for studies of other classes of enzymes that have protein substrates.

A thorough analysis of protease specificity can be used to produce suitable substrates and potent, selective inhibitors, as shown here with ICE. A fluorogenic substrate incorporating its preferred recognition motif, Ac-WEHD-AMC, is cleaved 50-fold more efficiently than that previously believed to be optimal for this enzyme, with a k_{cat}/K_m of $3.3 \times 10^6 \text{ M}^{-1}\text{s}^{-1}$. The corresponding peptide aldehyde, Ac-WEHD-CHO, appears to have an intrinsic K_i of $<10 \text{ pM}$, making this among the most potent reversible, peptide-based inhibitors described for any protease.

Having established that this method gives an accurate assessment of protease specificity, it can now be used to determine the amino-acid preferences of all caspase family members. Initial indications are that these enzymes have diverse biological roles, with essential functions in both inflammation and apoptosis. Information obtained with this library may help to further define the functional and evolutionary relationships between these proteases, and may provide important insights into the biological reactions that they mediate. In addition, these results should facilitate the design of selective inhibitors for caspases that are identified as potential therapeutic targets.

Materials and methods

Synthesis and characterization of positional-scanning library

As a representative example, the P₃ spatially addressed library was prepared as follows: *N*-allyloxycarbonyl-L-aspartic acid- α -AMC was loaded onto a Rapp Polymere TentaGel S NH₂ resin containing the 4-(4-hydroxymethyl-3-methoxyphenoxy)-butyric acid (HMPB) handle via the Mitsunobu reaction (diisopropyl azodicarboxylate (DIAD)/triphenylphosphine (TPP)). The allyloxycarbonyl (Alloc) group was removed using Pd(Ph₃)₄ and 1,3-dimethylbarbituric acid (DMBA) in dichloromethane (DCM). The isokinetic mixture of protected amino acids was then prepared by dissolving the requisite amounts of each monomer in *N,N*-dimethylacetamide (DMA) along with 1-hydroxybenzotriazole hydrate (HOBT) followed by addition of 1-(3-dimethylamino-propyl)-3-ethylcarbodiimide hydrochloride (EDC). The isokinetic mixture was added to the resin followed by agitation for 2 hours. The resin was washed with DMA and the procedure was repeated. The resin was washed with DMA, DCM and *N,N*-dimethylformamide (DMF). Elimination of the Fmoc (25% piperidine in DMF for 15 min) was followed by washing with DMA, tetrahydrofuran (THF), isopropyl alcohol (IPA) and DCM. The resin was transferred into 20 individual reaction vessels by the isopycnic slurry method [33] and washed with DMA. Position P₃ was 'spatially addressed' by pre-activating the 20 individual amino acids with EDC/HOBT as described above followed by addition to the 20 reaction vessels. After 2 h the resin was washed with DMA and the procedure repeated. After Fmoc removal and washing, P₄ was installed by adding the isokinetic mixture of amino acids to each vessel. Following Fmoc removal, the amino terminus was acetylated with Ac₂O/pyridine/DMF (1:2:3) for 1 h. The acetylation was repeated followed by washing with DMA, H₂O, THF, IPA and DCM. The resin bound mixtures were then twice cleaved for 30 min using trifluoroacetic acid (TFA)/H₂O/phenol (PhOH)/triisopropylsilane (TIS) (88:5:5:2). The cleavage solution was aged for 1 h and 20 min prior to solvent removal *in vacuo*. The tetrapeptide-AMC derivatives were twice precipitated from cold Et₂O before being lyophilized from CH₃CN/H₂O (2:1). The yields for the individual wells ranged from 30–49%. Each of the 60 samples were prepared as approximately 10 mM stocks in dimethyl sulfoxide (DMSO).

Preparation of individual, fluorogenic substrates

A representative procedure for single pure substrate synthesis is as follows: *N*-allyloxycarbonyl-L-aspartic acid- α -AMC was loaded onto a Rapp Polymere TentaGel S NH₂ resin containing the HMPB handle via the Mitsunobu (DIAD/TPP). After removal of the Alloc group using Pd(Ph₃)₄ and DMBA in DCM, *N*- α -Fmoc-*N*-im-trityl-L-histidine was coupled to the amine terminus using 2-(1H-benzotriazole-1-yl)-1,1,3,3-tetramethyluronium hexafluorophosphate (HBTU), HOBT, and *N,N*-diisopropylethylamine (DIPEA) in 1-methyl-2-pyrrolidinone (NMP). Elimination of the Fmoc (25% piperidine in DMF) was followed by coupling as above employing the requisite amino acids, in this case *N*- α -Fmoc-L-glutamic acid, γ -t-butyl ester and *N*- α -Fmoc-*N*-in-t-Boc-L-tryptophan, respectively. Fmoc was followed by acetylation with Ac₂O/pyridine/DMF (1:2:3). The desired substrate was cleaved from the

resin with TFA/H₂O/PhOH/TIS (88:5:5:2). Removal of the cleavage cocktail *in vacuo* was followed by precipitation from cold Et₂O. The amorphous solid was lyophilized from CH₃CN/H₂O (2:1) and purified via MPLC (Lobar LiChrorep RP-18; 25% CH₃CN/H₂O containing 0.1% TFA) to provide after lyophilization Ac-WEHD-AMC•TFA in 37% yield.

Synthesis and purification of Ac-WEHD-CHO

N- α -Fmoc-N-im-trityl-L-histidine was loaded onto a Rapp Polymere TentaGel S NH₂ resin containing the HMPB handle via the Mitsunobu reaction (DIAD/TPP). Elimination of the Fmoc (25% piperidine in DMF) was followed by coupling to N- α -Fmoc-L-glutamic acid γ -benzyl ester employing HBTU, HOBT and DIPEA in NMP. Removal of the Fmoc and coupling was repeated substituting N- α -Fmoc-N-im-t-Boc-L-tryptophan for N- α -Fmoc-L-glutamic acid γ -benzyl ester. Fmoc removal was followed by acetylation with Ac₂O/pyridine/DMF (1:2:3). The tripeptide was cleaved from the resin with TFA/H₂O/PhOH/TIS (88:5:5:2). Removal of the cleavage cocktail *in vacuo* was followed by precipitation from cold Et₂O. The amorphous solid was lyophilized from CH₃CN/H₂O (2:1) providing Ac-WE(OBzl)H-OH•TFA in 44% yield. A solution of N-Alloc-4-amino-5-benzoyloxy-2-oxotetrahydrofuran [34] and Ac-WE(OBzl)H-OH•TFA in DCM and DMF was first exposed to (PPh₃)₂PdCl₂ and tri-n-butyltin hydride, then cooled to 0°C and coupled employing EDC and HOBT. After allowing the reaction mixture to reach ambient temperature over 2 h, the crude reaction mixture was further diluted with DMF and purified via MPLC (Sephadex LH-20; DMF as the eluent). The DMF was removed *in vacuo* and the desired product was precipitated from Et₂O/hexane to provide N-(N-acetyltyrosinyl-glutamyl(OBzl)-histidinyl)-4-amino-5-benzoyloxy-2-oxotetrahydrofuran in 50% yield. Hydrogenation (20% Pd(OH)₂/CH₃OH/H₂ balloon) for one hour followed by purification via MPLC (Lobar LiChrorep RP-18; 15% CH₃CN/H₂O containing 0.1% TFA) provided after lyophilization Ac-WEHD-CHO•TFA in 45% yield.

Preparation of active ICE

The method used for production of recombinant protease involves folding of the active enzyme from its constituent large and small subunits which are expressed separately in *Escherichia coli*. The 20 kDa (p20) and 10 kDa (p10) subunits of ICE were individually expressed in *E. coli* BL21(DE3)pLysS cells and recombinant protein expression was induced by overnight growth in the presence of 1 mM IPTG. Cells were harvested, washed and broken in the presence of protease inhibitors then inclusion bodies were isolated and solubilized in 6 M guanidine-hydrochloride. To obtain active enzyme, the individual subunits were rapidly diluted to a final concentration of 100 mg ml⁻¹ at ambient temperature into a solution containing 100 mM Hepes, 10% sucrose, 10 mM DTT, 1% Trilon X-100, pH 7.5 and Sepharose-Ac-YVAD-CHO (0.05 ml resin/ml solution) [20,28]. After stirring the solution for three days the resin was harvested and washed exhaustively with 100 mM Hepes, 10% sucrose, 0.1% CHAPS, pH 7.5. The enzyme was eluted by treatment with 100 μ M Ac-YVAD-CHO for 24 h at ambient temperature. Inhibitor was removed by treatment with hydroxylamine and oxidized glutathione as described [28].

Table 3

Crystallographic data and refinement.

Data collection		Refinement	
No. reflections		rms deviation	
observed	26 257	of bonds	0.007 Å
unique	9705	of angles	1.39°
Completeness	87.0%	of dihedrals	24.02°
R _{merge}	4.7%	of improvers	1.20°
		R _{free}	28.8%
		R	18.4%

Measurement of kinetic constants

Measurement of k_{cat}/K_m for individual tetrapeptide-AMC substrates: Liberation of AMC from each substrate was monitored continuously in a Gilford Fluoro IV Spectrofluorometer using an excitation wavelength of 380 nm and an emission wavelength of 460 nm. Reactions were initiated by adding 10–60 nM enzyme to an assay mixture containing 0.5 μ M substrate in 100 mM Hepes, 10% sucrose, 0.1% CHAPS, 0.1% ovalbumin, 10 mM DTT, pH 7.5, and 25°C. Data were fit by non-linear regression to a first-order rate equation ($AMC = A \cdot \exp^{-k_{obs} \cdot t} + B$) to obtain the rate constant for hydrolysis of substrate ($k_{obs} = k_{cat} \cdot E / K_m$). This rate constant was corrected for enzyme concentration to produce values for k_{cat}/K_m .

Measurement of K_i for Ac-WEHD-CHO: The continuous, fluorometric assay employed for these studies has been previously described [20,28]. All reactions were performed under standard reaction conditions (standard reaction conditions) using homogeneous enzyme. Reactions were monitored continuously in a Gilford Fluoro-IV fluorometer using an excitation wavelength of 380 nm and an emission wavelength of 460 nm. To measure the association rate constant (k_{on}), enzyme was added to reaction mixtures containing 1 μ M Ac-YVAD-AMC and various concentrations of inhibitor. The dissociation rate constant (k_{off}) was determined by preincubation of enzyme and inhibitor (25 nM ICE, 125 nM Ac-WEHD-CHO), followed by 500-fold dilution into a reaction mixture containing 100 μ M levels of substrate. The overall dissociation constant, K_i , was calculated from the observed rates of association and dissociation according to the equations developed by Morrison for analysis of slow and tight-binding inhibitors [35].

Determination of ICE•WEHD-CHO crystal structure

The ICE•Ac-WEHD-CHO complex was crystallized by hanging-drop vapor diffusion. 1.5-ml drops of protein-inhibitor solution (5.0 mg ml⁻¹ in 10 mM Tris-HCl pH 8.5, 10 mM DTT, 3 mM Na₂S₂O₃) were mixed with an equal volume of reservoir buffer (7.2% PEG-6000 (w/w), 0.10 M PIPES pH 5.8, 10 mM DTT, 3 mM Na₂S₂O₃) and incubated at room temperature. The crystals belong to the tetragonal space group P4₃2₁2 with a=b=64.61, c=160.10 Å and are isomorphous with crystals of the ICE•Ac-YVAD-CHO complex grown under similar conditions (JR and JWB, unpublished observations). Three-dimensional diffraction data extending to a resolution of 2.73 Å were collected at room temperature using a Siemens area detector and CuK α radiation from a Rigaku RU-200 rotating-anode X-ray generator. These data were processed with the SAINT software package [34]. 25022 observations of 8445 unique reflections were merged with an R-factor of 4.70%. 67.3% of observations had $|F| > 2\sigma$ in the highest resolution shell, 2.73 < d < 2.83 Å. The structure was solved by difference Fourier methods, using a model based on the protein portion of the structure of ICE•Ac-YVAD-CHO (JR and JWB, unpublished observations). Unambiguous volunteer density for the inhibitor was evident in the initial electron density maps, and a model of the inhibitor was constructed by interactive model-building [35]. The resulting model was refined using X-PLOR [36] and all diffraction data with $|F| > 2\sigma$. In the later stages of refinement, the interpretation of the inhibitor and binding site models was confirmed by simulated-annealing omit maps [37]. For the final model, the crystallographic R-factor is 18.4% (R_{free}=28.8%), [38] with rms deviations from ideal values [39] of 0.007 Å in bond lengths and 1.39° in bond angles. Crystallographic statistics are presented in Table 3 and representative electron density is shown in Figure 3e.

Accession numbers

The coordinates and structure factors of the ICE•Ac-WEHD-CHO complex have been deposited in the Protein Data Bank [40] and the PDB code is 1IBC.

References

1. Matthews, D.J. & Wells, J.A. (1993). Substrate phage: selection of protease substrates by monovalent phage display. *Science* **260**, 1113–1117.

2. Matthews, D.J., Goodman, L.J., Gorman, C.M. & Wells, J.A. (1994). A survey of furin substrate specificity using substrate phage display. *Prot. Science* **3**, 1197–1205.
3. Smith, M.M., Shi, L. & Navre, M. (1995). Rapid identification of highly active and selective substrates for stromelysin and matrilysin using bacteriophage peptide display libraries. *J. Biol. Chem.* **270**, 6440–6449.
4. Meldal, M., Svendsen, I., Breddam, K. & Auzanneau, F.-I. (1994). Portion-mixing peptide libraries of quenched fluorogenic substrates for complete subsite mapping of endoprotease specificity. *Proc. Natl Acad. Sci. USA* **91**, 3314–3318.
5. Petithory, J.R., Masiarz, F.R., Kirsch, J.F., Santi, D.V. & Malcolm, B.A. (1991). A rapid method for determination of endoprotease substrate specificity: Specificity of the 3C proteinase from hepatitis A virus. *Proc. Natl Acad. Sci. USA* **88**, 11510–11514.
6. Berman, J., et al., & Wiseman, J. (1992). Rapid optimization of enzyme substrates using defined substrate mixtures. *J. Biol. Chem.* **267**, 1434–1437.
7. Schellenberger, V., Turck, C.W., Hedstrom, L. & Rutter, W.J. (1993). Mapping the S' subsites of serine proteases using acyl transfer to mixtures of peptide nucleophiles. *Biochemistry* **32**, 4339–4353.
8. Pinilla, C., Appel, J.R., Blanc, P. & Houghten, R.A. (1992). Rapid identification of high affinity peptide ligands using positional scanning synthetic peptide combinatorial libraries. *Biotechniques* **13**, 901–905.
9. Ostresh, J.M., Winkle, J.H., Hamashin, V.T. & Houghten, R.A. (1994). Peptide libraries - determination of relative reaction-rates of protected amino acids in competitive couplings. *Biopolymers* **34**, 1681–1689.
10. Dooley, C.T. & Houghten, R.A. (1993). The use of positional scanning synthetic peptide combinatorial libraries for the rapid-determination of opioid receptor ligands. *Life Sci* **52**, 1509–1517.
11. Wallace, A., et al., & Pessi, A. (1994). A multimeric synthetic peptide combinatorial library. *Pept. Res.* **7**, 27–31.
12. Owens, R.A., Gesellchen, P.D., Houchins, B.J. & DiMarchi, R.D. (1991). The rapid identification of HIV protease inhibitors through the synthesis and screening of defined peptide mixtures. *Biochem. Biophys. Res. Commun.* **181**, 402–408.
13. Eichler, J. & Houghten, R.A. (1993). Identification of substrate-analog trypsin inhibitors through the screening of synthetic peptide combinatorial libraries. *Biochemistry* **32**, 11035–11041.
14. Pinilla, C., et al., & Houghten, R.A. (1994). Versatility of positional scanning synthetic combinatorial libraries for the identification of individual compounds. *Drug Devel. Res.* **33**, 133–145.
15. Eichler, J., Lucka, A.W. & Houghten, R.A. (1994). Cyclic peptide template combinatorial libraries: Synthesis and identification of chymotrypsin inhibitors. *Pept. Res.* **7**, 300–307.
16. Pinilla, C., Appel, J.R. & Houghten, R.A. (1994). Investigation of antigen-antibody interactions using a soluble, non-support-bound synthetic decapeptide library composed of four trillion (4×10^{12}) sequences. *Biochem. J.* **301**, 847–853.
17. Black, R.A., Kronheim, S.R. & Sleath, P.R. (1989). Activation of interleukin-1 β by a co-induced protease. *FEBS Lett.* **247**, 386–390.
18. Kostura, M.J., et al., & Schmidt, J.A. (1989). Identification of a monocyte specific pre-interleukin 1 β convertase activity. *Proc. Natl Acad. Sci. USA* **86**, 5227–5231.
19. Cerretti, D.P., et al., & Black, R.A. (1992). Molecular cloning of the interleukin-1 β converting enzyme. *Science* **256**, 97–100.
20. Thornberry, N.A., et al., & Tocci, M.J. (1992). A novel heterodimeric cysteine protease is required for interleukin-1 β processing in monocytes. *Nature* **356**, 768–774.
21. Kuida, K., et al., & Flavell, R.A. (1995). Altered cytokine export and apoptosis in mice deficient in interleukin-1 β converting enzyme. *Science* **267**, 2000–2003.
22. Li, P., et al., & Seshadri, T. (1995). Mice deficient in IL-1 β -converting enzyme are defective in production of mature IL-1 β and resistant to endotoxic shock. *Cell* **80**, 401–411.
23. Yuan, J., Shaham, S., Ledoux, S., Ellis, H. M. & Horvitz, H. R. (1993). The *C. elegans* cell death gene *ced-3* encodes a protein similar to mammalian interleukin-1 β -converting enzyme. *Cell* **75**, 641–652.
24. Alnemri, E.S., et al., & Yuan, J. (1996). Human ICE/CED-3 protease nomenclature. *Cell* **87**, 171.
25. Kuida, K., et al., & Flavell, R.A. (1996). Decreased apoptosis in the brain and premature lethality in CPP32-deficient mice. *Nature* **384**, 368–372.
26. Sleath, P.R., Hendrickson, R.C., Kronheim, S.R., March, C.J. & Black, R.A. (1990). Substrate specificity of the protease that processes human interleukin-1 β . *J. Biol. Chem.* **265**, 14526–14528.
27. Howard, A. D., et al., & Tocci, M.J. (1991). IL-1-converting enzyme requires aspartic acid residues for processing of the IL-1 β precursor at two distinct sites and does not cleave 31 kDa IL-1 α . *J. Immunol.* **147**, 2964–2969.
28. Thornberry, N.A. (1994). Interleukin-1 β converting enzyme. *Methods Enzymol.* **244**, 615–631.
29. Thornberry, N.A. & Molineaux, S.M. (1995). Interleukin-1 β converting enzyme: A novel cysteine protease required for IL-1 β production and implicated in programmed cell death. *Protein Sci.* **4**, 3–12.
30. Rich, D.H. (1986). Inhibitors of cysteine proteinases. In *Proteinase Inhibitors*. (Barrett, A.J. & Salvesen, G. eds) pp.153–178. Elsevier, Amsterdam.
31. Wilson, K. P., et al., & Livingston, D.J. (1994). Structure and mechanism of interleukin-1 β converting enzyme. *Nature* **370**, 270–275.
32. Walker, N.P.C., et al., & Wong, W.W. (1994). Crystal structure of the cysteine protease interleukin-1 β -converting enzyme: A (p20/p10) $_2$ homodimer. *Cell* **78**, 343–352.
33. SAINT Software Reference Manual. (1995). Siemens Analytical Instruments, Madison, Wisconsin.
34. Sack, J.S. (1988). CHAIN - A crystallographic modeling program. *J. Mol. Graphics* **6**, 224–225.
35. Morrison, J.F. & Walsh, C.T. (1988). *Adv. Enzymol. Relat. Areas Mol. Biol.* **61**, 201–301.
36. Brünger, A.T. (1992). X-PLOR: Version 3.1, a System for X-Ray crystallography and NMR. Yale University Press, New Haven & London.
37. Hodel, A., Kim, S.-H. & Brünger, A.T. (1992). Model bias in macromolecular crystal structures. *Acta Crystallogr.* **A48**, 851–858.
38. Brünger, A.T. (1992). Free R Value: a novel statistical quantity for assessing the accuracy of crystal structures. *Nature* **355**, 472–475.
39. Engh, R.A. & Huber, R. (1991). Accurate bond and angle parameters for X-ray protein structure refinement. *Acta Cryst.* **A47**, 392–400.
40. Abola, E.E., Bernstein, F.C., Bryant, S.H., Koetzle, T.F. & Weng, J. (1987). Protein Data Bank. In *Crystallographic Databases - Information Content, Software Systems, Scientific Applications*. (Allen, F.H., Bergerhoff, G. & Sievers, R. eds) pp. 107–132, Data Commission of the International Union of Crystallography, Bonn/Cambridge/Chester.